Journal of Nuclear Materials 381 (2008) 216–222

Contents lists available at ScienceDirect

Journal of Nuclear Materials

journal homepage: www.elsevier.com/locate/jnucmat

Predicted mechanisms for radiation enhanced helium resolution in uranium dioxide

David C. Parfitt, Robin W. Grimes *

Department of Materials, Imperial College London, London SW7 2AZ, UK

ARTICLE INFO

Article history:
Received 23 April 2008
Accepted 13 June 2008

ABSTRACT

Classical molecular dynamics has been performed to predict the behaviour of helium gas bubbles in uranium dioxide, UO_2, when subjected to displacement cascades that mimic the effects of self-irradiation damage. The models presented here examine bubble sizes of 2 and 4 nm with several different gas densities and displacement cascades with energies of up to 50 keV. Of particular interest are the mechanisms by which helium atoms can be returned to solution in the lattice through interaction with displacement cascades. This occurs both via ballistic recoil from high-energy ion fragments traversing the bubble and also a damage assisted resolution whereby the high-pressure gas intermixes into the disordered cascade regions formed adjacent to the surface of the bubble.

1. Introduction

Helium is formed in uranium dioxide, UO_2, as a consequence of the α-decay of actinides during both normal reactor operation and the long-term storage of nuclear fuel. The helium atoms, together with insoluble fission gasses such as krypton and xenon, precipitate into microscopic bubbles of gas within the UO_2 lattice [1–5]. Understanding the behaviour of these bubbles is important as the bubbles become associated with microstructural defects and cause degradation of the fuel's mechanical and thermal properties [4,6,7]. The accumulation of helium gas bubbles at grain boundaries can lead to a loss of cohesion amongst the grains [8], reducing the fuel pellets into powder. In addition, the growth and eventual interlinkage of bubbles can produce an extended network of pores and a rapid release of gas into the surrounding environment [4,7,9–12].

In this paper we will consider mechanisms by which helium may be returned from the bubbles back into solution within the lattice. Understanding this process is crucial in determining the equilibrium density and sizes of the bubbles [1,13,4,5] as well as their migration rate [14,15,1,3,16–18]. The resolution of helium may occur from thermal effects, although at normal fuel operating and storage temperatures this is thought to make a small contribution to the total resolution rate [19,13]. Alternatively gas may re-enter the lattice through radiation-enhanced resolution [20–22]. In this second process helium atoms are returned to the lattice by the interaction of the bubbles with energetic recoil cascades initiated by fission or α-decay events within the nuclear fuel.

Previous empirical models of radiation-enhanced gas resolution [21,22] have assumed that gas is redistributed into the lattice by means of energetic recoil from high-energy ion fragments traversing the bubble. Atoms are assumed to have redissolved into the lattice if they collide with the surface of the bubble with a kinetic energy greater than some threshold energy E_{min}, which corresponds to the energy necessary to place the atom sufficiently far from the influence of the bubble that re-precipitation of the gas does not immediately occur. Gas atoms may acquire this threshold energy via direct interaction with the fission fragments, or for bubbles with a high gas density, by secondary collisions with other gas atoms. These two processes lead to a resolution rate that is dependent upon the probability of a helium atom encountering such a energetic fragment within the bubble.

Empirical models of the resolution of gas atoms from bubbles are able to give good quantitative values for levels of gas resolution. However, the many different physical processes that also contribute to the equilibrium size and mobility of the gas bubbles have complicated the physical interpretation of radiation-enhanced resolution. As a first step in understanding the atomistic scale processes that occur during resolution, we present this study of the interaction of helium gas bubbles with recoil cascades that are representative of nuclear processes within the fuel. We consider only helium gas despite the importance of xenon and krypton fissions products. Due to its low polarisability, helium is known to be well modelled using classical molecular dynamics [2]. It is our intention to consider other insoluble gasses in subsequent studies.

On a microscopic level it is possible to simulate the process of helium resolution as a function of several variables including deposited energy, bubble volume, lattice temperature, gas pressure within the bubble, bubble geometry, direction of the initial primary knock-on atom, resulting cascade morphology and gas composition (i.e., Xe/Kr/He ratios). Clearly there are numerous variables that one would want to persue. We concentrate here on the effects of the overall size of the bubble and internal gas pressure (which, for small bubbles, is ill-determined experimentally and theoretically). The morphology of the bubble before relaxation

* Corresponding author. Tel.: +44 20 7594 6730.
E-mail address: r.grimes@imperial.ac.uk (R.W. Grimes).

0022-3115/$ - see front matter © 2008 Elsevier B.V. All rights reserved.
doi:10.1016/j.jnucmat.2008.06.038

is spherical, although we have observed a similar range of resolution processes from octahedral-shaped bubbles bounded by the lowest energy (1 1 1) surfaces [23]. Finally we have carried out each simulation at a lattice temperature of 800 K, as representative of a temperature experienced within a fuel pin of an operational nuclear reactor.

The results are consistent with the previous view that thermal resolution of the helium gas is almost negligible up to standard fuel operating temperatures [19,13]. We examine two different bubble sizes as specific examples showing several new physical processes that occur during the interaction of gas bubbles with recoil cascades. These processes may dramatically impact upon the resolution rate of the helium back into the lattice, the migration and equilibrium populations of the bubbles and the rate at which the gas-infiltrated disordered lattice recovers its crystal structure. Finally, we present a statistical study of the rate of resolution as a function of the internal gas density for a bubble diameter of 4 nm.

2. Methodology

To study the dynamic behaviour of helium bubbles in UO_2, we have carried out a series of classical molecular dynamics simulations. Simple two-body potentials are used to model the interaction between uranium and oxygen ions and the helium atoms [2,24]. The requirements of these potentials are that they should be computationally tractable, they should replicate the long-range structure of uranium dioxide and they should be robust enough to handle the energetic collisions seen in recoil cascades.

To perform the simulations, the code DL_POLY version 3.02 [25] was used; details of the operation of this code are given elsewhere [26]. We employed the variable timestep option which scales the integration timestep at each simulation frame depending upon the maximum distance an ion is allowed to move. This allowed an efficient sampling of the dynamical behaviour of the simulation both during the energetic displacement cascade and in the longer timescale equilibration periods.

Simulations were run in a constant-pressure, constant-temperature (NPT) ensemble to establish the equilibrium cell metric; a constant-volume, constant-temperature (NVT) ensemble during the pre- and post-cascade equilibration period and a constant-volume constant-energy (NVE) ensemble for the brief displacement cascade period where the system was far from thermal equilibrium. A Berendsen thermostat [27] was used to correct the temperature, and where appropriate the pressure, with a relaxation time of 0.1 ps.

Recoil cascades produce large-scale disorder in a pure crystal lattice. In the finite system sizes considered here, typically $20 \times 20 \times 20$ unitcells, it is possible for the resulting cascade disorder to interact with periodic images of itself. To minimise this interaction a heat bath was embedded in the walls of each simulation box. This consisted of a 0.3 nm thick layer of atoms, the velocities of which were coupled to a Langevin thermostat [28]. The layer was effective at absorbing the thermal spike and any high-energy atoms released by the cascade, thereby effectively embedding the central region in an infinite surrounding crystal.

2.1. Potential models

As we are dealing with an ionic solid the interactions between ions are separated into a Coulombic part, which represents the interaction between point charges, and a short-range energy. The comparatively long range Coulombic part of the interaction is computed internally in the DL_POLY code via a smooth particle mesh Ewald sum [29]. This ensures both accurate convergence of the Coulombic part of the energy and efficient dissemination of the computational cost over several parallel processors. For the calculation of the Coulombic interaction energy, the uranium and oxygen ions both assume their full, formal charges of +4 and −2, respectively.

The remaining short-range interaction energies, $V_{ij}(r)$, between pairs of ions i and j separated by a distance r, are represented by potentials taken from the literature (see Table 1) and are as follows.

The interaction between U^{4+} and O^{2-} ions [2] is modelled using the Buckingham potential of the form

$$V_{ij}(r) = A_{ij} \exp\left(-\frac{r}{\rho_{ij}}\right) - \frac{C_{ij}}{r^6}, \tag{1}$$

where A_{ij}, ρ_{ij} and C_{ij} are empirically determined parameters.

The interaction between helium atoms and U^{4+} and O^{2-} ions is described by a Lennard–Jones potential of the form

$$V_{ij}(r) = 4\epsilon_{ij}\left[\left(\frac{\sigma_{ij}}{r}\right)^{12} - \left(\frac{\sigma_{ij}}{r}\right)^{6}\right], \tag{2}$$

where ϵ and σ are parameters derived from Hartree—Fock calculations of helium atoms in UO_2 [2].

Finally, to account for the interactions between pairs of helium atoms (particularly important in the bubble) we used a potential of the form [24]

$$V_{ij}(r) = A \exp\left(-\alpha r - \beta r^6\right) - \frac{0.869}{\left(r^2 + a^2\right)^3}\left(1 + \frac{2.709 + 3a^2}{r^2 + a^2}\right), \tag{3}$$

where A, a, α and β are parameters derived from empirical fits to high-energy collisions of helium atoms to separations of only 50 pm but the potential is also able to replicate the low-density behaviour of a helium gas.

The short range interatomic potentials described so far, for interactions involving ionic species, were derived to model the region of interatomic separation around equilibrium and are not necessarily appropriate for modelling the violent collisions that occur during displacement cascades. To remove this deficiency a Ziegler–Biersack–Littmark (ZBL) model potential [30] was used to replicate the high-energy, low-separation part of the potentials; this models the reduction in electronic shielding between two nuclei due to the distortion of the electron shells as the ions are brought closer together.

To join the high-energy ZBL functions and the low-energy Buckingham parts of the potentials, fifth-order polynomial splines were used. The polynomial coefficients were obtained through the requirement that the potential energy of each ion-pair (that is, the short-range *plus* Coulombic energy) and its first and second derivatives should be continuous at the boundaries of the transition region and that the polynomial function should decrease monotonically throughout the transition region. The extent of the transition region is delineated by two additional parameters r_1 and r_2, the values of which are given for each ion pair in Table 1.

2.2. Construction of the bubbles of helium gas

The construction of the bubbles and the simulation of their interaction with damage cascades was realised in a number of steps.

2.2.1. Equilibration of a perfect crystalline uranium dioxide lattice

Firstly perfect crystalline UO_2 was simulated using a $20 \times 20 \times 20$ supercell of the reported crystal structure [31] as the starting configuration; this simulation was run for 25 000 timesteps (~50 ps) in an NPT ensemble to ensure the crystal had time to sample a suitable local average of equilibrium structures at a given temperature and pressure. The distribution of ionic velocities

Table 1
Potential parameters used for the short range interactions between U^{4+} and O^{2-} ions and He atoms

Buckingham potential					**Trans. region**	
	A (eV)	ρ (nm)	C (eV nm^6)		r_1 (nm)	r_2 (nm)
U–U	18600.0	2.746×10^{-2}	3.264×10^{-5}		5×10^{-2}	0.1
U–O	2494.2	3.4123×10^{-2}	4.016×10^{-5}		7×10^{-2}	0.12
O–O	108.0	3.8×10^{-2}	5.606×10^{-5}		6×10^{-2}	0.15
Lennard–Jones potential						
	ϵ (eV)	σ (nm)				
He–U	2.7106×10^{-2}	0.49505			–	–
He–O	1.5386×10^{-2}	0.24000			–	–
Helium–helium potential						
	A (eV)	a (nm)	α (nm^{-1})	β (nm^{-6})		
He–He	398.7	6.75×10^{-2}	43.90	3.746×10^2	2×10^{-2}	5×10^{-2}

was rescaled during the first 5000 timesteps. From this equilibrium structure the average supercell metric was calculated over the last 20 000 timesteps, the remaining simulations were carried out at an NVT ensemble, constrained to this average supercell size.

2.2.2. Construction of the bubble

Bubbles were inserted into the simulated UO_2 crystal by first removing a stoichiometric number of uranium and oxygen ions from a central spherical region to form a void within the crystal. Helium atoms from a separate simulation of helium gas at a predetermined pressure and temperature were then introduced into this void. Finally the UO_2 crystal with the new helium gas bubble was allowed to equilibrate for a total of 25 000 timesteps (~50 ps), in order to allow the excess potential energy of the freshly cleaved surface and the helium–surface interactions to dissipate.

Relaxation of the spherical gas bubbles produced a final bubble shape that was slightly faceted – in agreement with the dominance of the (1 1 1) plane [32,14,23] for large equilibrium gas bubbles.

2.2.3. Recoil cascades

Radiation cascades were modelled by selecting a U^{4+} ion and assigning to it an additional kinetic energy, corresponding to a recoil event within the crystal. The velocity of this recoil was directed towards the centre of the gas bubble and the recoil ion position was chosen such that the cascade should have sufficient distance to transfer energy to several other ions by the time it reached the bubble surface. This is the principle consideration of the present study; that the energy of the recoil process is deposited in a region of the lattice adjacent to and intersecting a bubble. Cascades that deposited their energy in a region adjacent but not intersecting a bubble were also studied but it was found that the crystal recovered (crystallised) before gas migrated from the bubble to the disordered region and these are not reported here.

2.2.4. Final equilibration

The radiation cascade and its interaction with the bubble was simulated for up to 50 000 timesteps (~25 ps). The peak damage occurred within the first fractions of a picosecond, however, we followed the relaxation of the lattice to much longer timescales in order to investigate the recovery processes.

2.3. Pressure in the helium bubble

For the simulations considered here we have examined a range of different internal gas pressures. We report for each simulation the number of helium atoms per formula unit of UO_2 removed to form the bubble. This removes any ambiguity in our reported results caused both by the relaxed volume occupied by the gas bubble and the conversion from this density to a final internal bubble pressure, as used in similar studies for helium bubbles in metals [33].

We also provide an estimate of the pressure in each bubble by comparing to the pressure obtained in a simulation of an equivalent density and temperature of free helium gas. Such a calculation neglects several important factors including: density fluctuations that ocur near the gas–crystal interface and deviations from ideal gas behaviour (see reference [34] for a more detailed discussion). Nevertheless the estimate provides an order of magnitude value. Using this calculation the pressure range we consider in these simulations is between 22 and 200 MPa. This covers the range of estimated helium pressures present either in the UO_2 fuel plenum or grain boundary bubbles at the end of life [35–37] or in long term storage [38,8]; direct measurements of implanted helium bubbles have examined helium atom concentrations similar to these [5,9,4]. Due to its lower production rate, higher solubility and higher mobility in a fuel matrix, the pressure of helium is considerably less in UO_2 than the several GPa pressures reported for krypton or xenon bubbles [39,40].

3. Results

We begin with a discussion of a 10 keV cascade occurring near a small 2 nm diameter bubble with a high helium to UO_2 vacancy ratio of 3.12 helium atoms per UO_2 formula unit (328 helium gas atoms in total). In Fig. 1, we show a series of four key snapshots taken from this recoil cascade over the first 8 ps of the simulation. By looking first at this example of a high-pressure helium bubble, where resolution events occur much more readily, we can establish some processes that result in resolution, and this commentary will support much of the following discussion.

3.1. Example of a cascade

Upon initiation of the cascade (Fig. 1(a)) the primary knock-on ion undergoes several high-energy collisions to produce a cascade of energetic ions. These travel towards the bubble causing considerable disruption of the UO_2 lattice. This damage field progresses until it intersects with the bubble. At this point a proportion of the cascade energy can be transferred to the gas atoms. Only a very few helium atoms are knocked out directly into the UO_2 lattice as a result of energetic collisions with atoms within the bubble. One such "recoil" helium, produced by direct collision with an energetic U^{4+} ion, is labelled in Fig. 1(b).

The process of resolution does not solely occur by the implantation of high-energy helium atoms deep into the crystal lattice, rather as shown in Fig. 1(b), it also is an intermixing of the high-pressure helium gas into the disordered region immediately adjacent to the bubble. Significantly, the lack of crystalline order of this region presents a much lower barrier (E_{min} in the nomenclature of

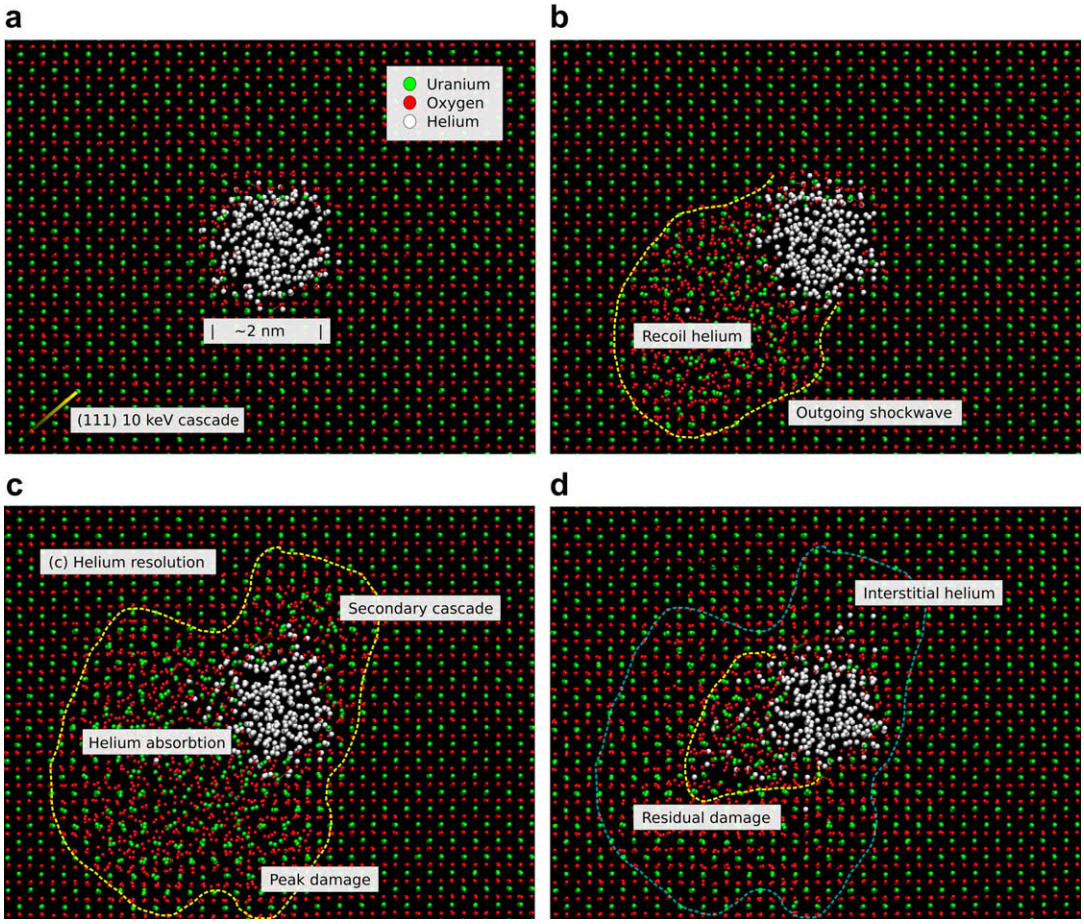

Fig. 1. A series of snapshots showing instantaneous ion positions for the interaction of a helium bubble with a 10 keV recoil cascade. Uranium ions are plotted in green, oxygen in red and helium atoms in white: (a) Cascade initiation (t = 0.0 ps): A 10 keV recoil atom is initiated in the lower left corner of the figure; (b) Ballistic shock phase (t = 0.8 ps): High-energy uranium and oxygen ions knock helium atoms into the disordered region; (c) Helium resolution (t = 1.2 ps): Helium atoms from the bubble leak into the damaged region and migrate through it. The yellow dotted line shows the peak area of recoil damage resulting from the cascade; (d) Final configuration (t = 8.0 ps): An area (outlined in yellow) of disordered UO_2 and helium atoms is formed from the result of the cascade. The blue dotted line illustrated the peak damage as shown in Fig. 1c.

Ronchi [21,22]) to the incorporation of helium from the bubble, than does the crystalline bubble surface. The existence of the disordered region is crucial as it provides an energetically accessible pathway for helium resolution.

Once removed from the bubble, the helium in the disordered region has a relatively high mobility, allowing it to be transported rapidly through this region. At the same time as the helium is moving into this region, the thermal energy from the recoil cascade has dissipated and the lattice is starting to recrystallise, from the edge of the disordered region inwards (between Figs. 1(c) and 1(d)). Where the recrystallisation front meets a low concentration of helium atoms, these are trapped, usually into octahedrally coordinated interstitial or U^{4+} substituted positions, although we have also observed helium atoms substituting on to tetrahedrally coordinated sites (usually occupied by O^{2-} ions). For higher concentrations of helium the recrystallisation front is halted; that is the helium atoms prevent further recovery of the lattice. Fig. 1(d) shows an example of this residual damage.

The evolution of the high helium content disordered region was simulated to 25 ps. No significant level of recrystallisation was observed, though given the highly-ionic nature of uranium dioxide it is unlikely that there will be any residual amorphisation given full thermal equilibrium [41,42]. It is not clear on these timescales the eventual fate of the helium atoms. There are three possibilities: (i) They may be re-incorporated into the bubble; (ii) they may be accommodated into crystalline sites within the recrystallised UO_2 lattice, or (iii) they may nucleate a second bubble adjacent to the first.

3.2. Time dependence of helium resolution

Next we examined the resolution rate from larger 4 nm bubbles across a wide range of internal gas densities suggested from experimental data [39,40]. For a 10 keV cascade the resolution from these bubbles was much smaller (in terms of fraction of gas resolved), often only consisting of a few atoms of helium. To increase the resolution rate we therefore employed a PKA of energy 50 keV, which produced much larger areas of disorder on the surface of the bubble.

Fig. 2 reports the evolution of a 50 keV cascade occurring adjacent to a 4 nm bubble. In this case the bubble contains 1712 atoms of helium equivalent to a density of 2.08 He per UO_2 formula unit. The lattice disorder (Fig. 2, y-axis) is defined as the number of original U^{4+} crystal sites from a time-average of the structure before the cascade took place, that subsequent to the cascade do not have a U^{4+} ion within 0.1 nm; before the cascade there is a small level of disorder due to ions that have moved around on the surface of the bubble (hence the graph in the upper portion of Fig. 2 does not show zero disorder at the start of the cascade). Given this definition, the upper portion of Fig. 2 shows that disorder in the simulation increases rapidly to a peak around 0.4 ps after cascade initiation. Subsequently it decays away to a level slightly above the original disorder in the UO_2 crystal.

There are a number of measures that could be employed to monitor lattice disorder. The method used here, based on the number of U^{4+} ions close to U^{4+} lattice sites, has the advantage that after

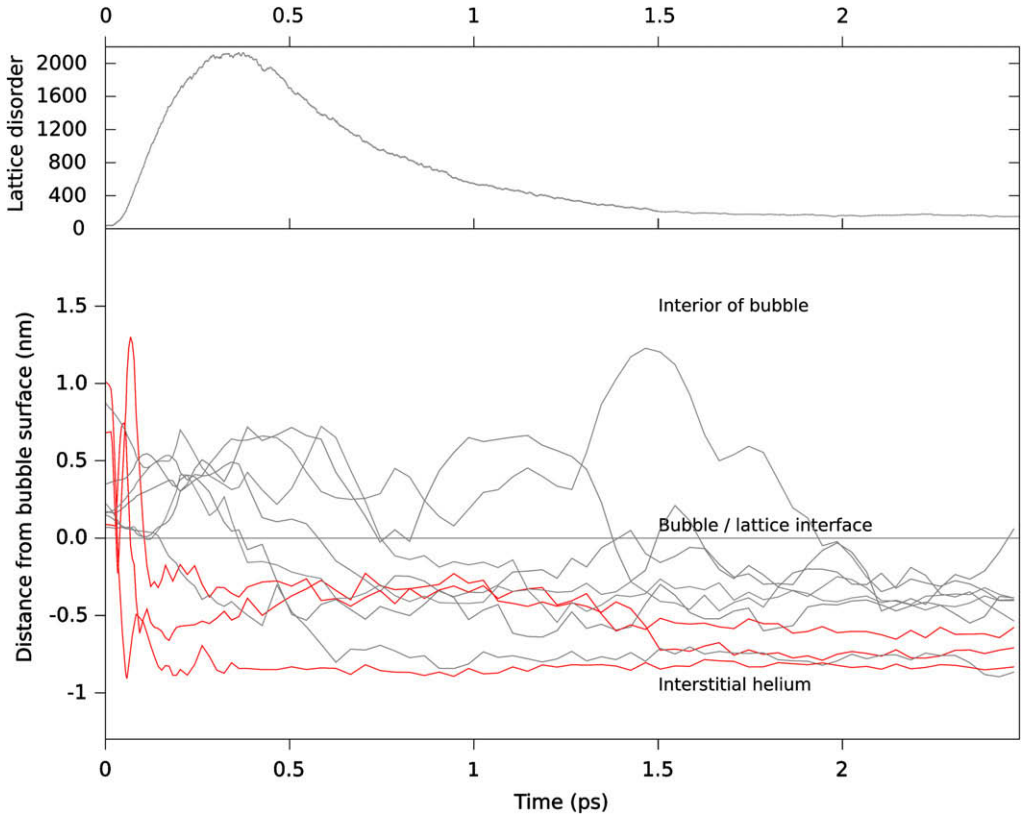

Fig. 2. A plot showing the evolution with time of a 4 nm diameter bubble subject to a 50 keV recoil cascade. The top plot shows the lattice damage measured as a function of vacant U^{4+} sites. The bottom plot shows the displacement of all the helium atoms that leave the bubble during the course of the simulation.

the lattice has recovered, a site is occupied (i.e. not contributing to the measure of lattice disorder) irrespective of which U^{4+} is adjacent to the site. That is, re-arrangement of the U^{4+} ions do not cause an increase in the amount of disorder. A disadvantage of this technique is that any disorder created independently on the O^{2-} sublattice is ignored.

The majority of helium atoms are unaffected by the cascade damage. However, as shown in Fig. 2, a few atoms are transferred from the bubble and deposited within the disordered UO_2 lattice. As time evolves and the lattice recovers, these atoms occupy octahedral or tetrahedrally coordinated sites within the lattice. These interstitial atoms are separated by several lattice spacings from the main helium bubble and do not move back into the bubble over the timescale of the simulations. Unlike the small, high-pressure bubble shown in Fig. 1 we did not observe any significant residual disordered regions at the end of the simulations.

We note that although the absolute rates of resolution as a fraction of total gas atoms have dropped significantly from the case of the smaller bubble shown in Fig. 1, there are still a number of atoms that leave the gas bubble at times that are significantly beyond the peak damage. We now divide the total number of gas atoms into three categories: atoms that remain within the bubble, atoms that escape the bubble through ballistic recoil and finally atoms that escape the bubble through resolution into defective regions adjacent to the surface of the bubble. Atoms that are resolved through either mechanism are defined as those whose position is greater that 2.25 nm from the centre of the bubble (0.25 nm from the bubble surface) in a period of time between 2.0 and 2.5 ps after the initiation of the displacement cascade. This definition neglects two sub-categories – resolved atoms that occupy stable lattice sites in the 0.25 nm boundary region at the bubble surface and non-resolved atoms that re-precipitate into the lattice at times greater that 2.5 ps. This definition is likely a pessimistic estimate of the absolute levels of resolution: from Fig. 2 we can see that there are atoms that appear to remain in the lattice on the lifetime of the simulation yet would not be counted towards the total resolution rate. The reprecipitation rate of helium atoms in lattice sites is, by contrast, a slow process; although in theory all of the resolved atoms shown will eventually either precipitate back into the bubble or move outwards into the crystalline bulk.

We now turn to the division of the resolved helium atoms into recoil and damage assisted resolution. Fig. 3 presents a plot of the atomic speeds of the same atoms shown in Fig. 2. The helium atoms shown fall into two categories: The upper three atoms (highlighted in red) that obtain speeds that are improbable to occur in normal thermal equilibrium of the bubble at the lattice temperature prior to the cascade initiation, and the lower atoms which always exhibit speeds well within the equilibrium distribution of speeds. On this basis, we consider an atom to have undergone ballistic recoil resolution if it has been resolved into the lattice (as defined above) and obtained, at anytime during the 2.5 ps of the simulation, a speed in excess of 20 km/s; the resolved atoms that stay below this limit are assumed to have undergone resolution through the damage assisted mechanism. Thus, in Figs. 2 and 3 the atoms which undergo recoil resolution are highlighted in red.

The value of speed used to define the division of resolved atoms into recoil and damage assisted categories is not unique. In particular ballistic resolution will exhibit a range of recoil energies. Even in our mono-energetic cascades occurring close to the surface of the bubble we observe a range of ballistic energies. In a real gas bubble with a range of initial PKA energies there will be a continuous spread of ballistic recoil processes down to energies which are comparable with those which occur well within a normal thermal distribution.

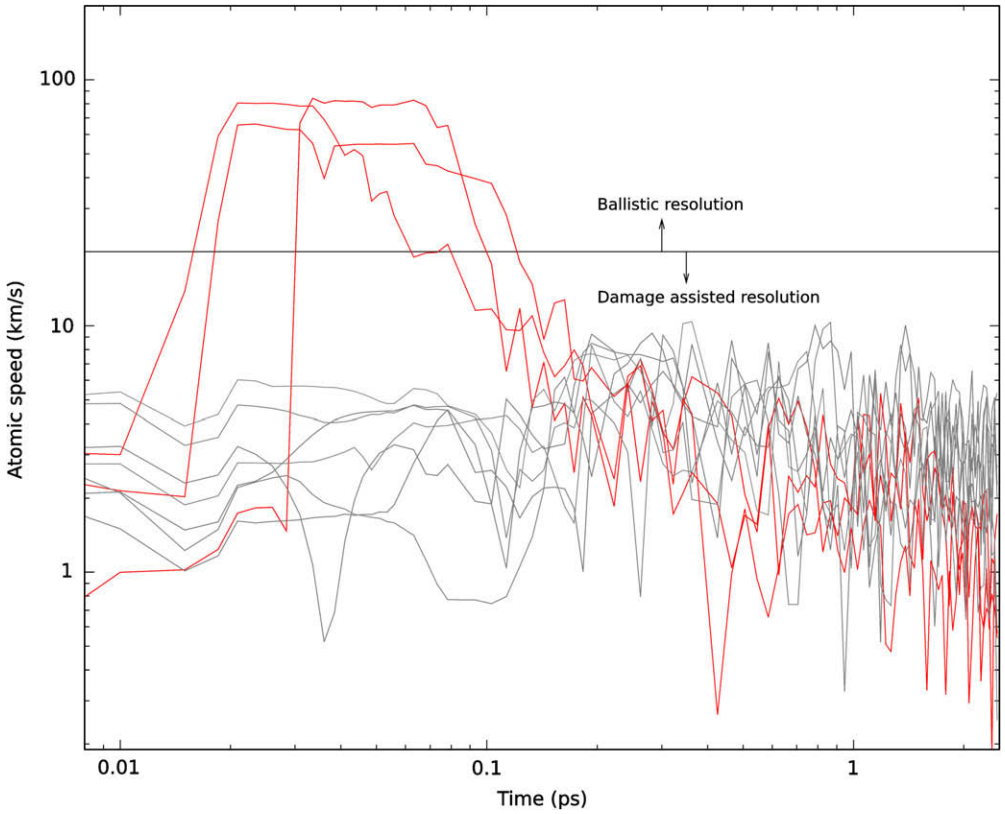

Fig. 3. A plot showing the evolution of the speeds of a selection of helium atoms during the course of a 50 keV cascade occurring near a 4 nm helium gas bubble. The selection of atoms is the same as in Fig. 2. Highlighted in red are the helium atoms which exceed the 20 km/s boundary between ballistic and damage assisted resolution. For comparison the root mean squared speed of helium atoms in thermal equilibrium at 800 K is approximately 2.3 km/s.

3.3. Effect of internal gas pressure

We now consider how the overal resolution rate changes as a function of the internal gas density. To achieve this we have taken the larger 4 nm bubble and removed different numbers of helium atoms. Each of these new densities was then allowed to equilibrate for around 10 ps.

The random nature of the morphology of the displacement cascades means it is not possible to predict in a deterministic way the amount of energy reaching the bubble surface and causing resolution, we adopt therefore a statistical analysis based on six equivalent cascade simulations. Thus, at each bubble pressure, we select six uranium ions within a distance of 3.5–3.8 nm from the centre of the bubble and give these ions a momentum directed towards the centre of the bubble corresponding to a kinetic energy of 50 keV. The number of resolved helium atoms from each of these simulations is averaged to obtain an estimate of the rate of resolution.

Table 2 shows the averaged results for these simulations together with the associated standard deviations in each case. The levels of resolution drop significantly as a function of the decreasing gas pressure. In the higher pressure bubbles resolution clearly occurs at a statistically significant level while at lower pressures the average number of resolved atoms per cascade drops below one. As discussed in the previous section, helium gas resolution occurs both during the ballistic damage phase and afterwards in the lattice recovery phase. The distinction is true at all but the lowest pressures studied. More work is need to determine whether the balance between ballistic and thermal resolution changes as a function of internal bubble pressure.

4. Discussion and conclusions

Results have been presented for a series of molecular dynamics simulations that model the interaction of helium gas bubbles in UO_2 with radiation cascades within the crystal lattice. In agreement with experimental and theoretical work we observe no thermal resolution from the bubble to the lattice prior to any interaction with the displacement cascade. However, we have identified two distinct mechanisms responsible for radiation enhanced resolution: (i) ballistic recoil resolution, which occurs as a result of collisions between helium atoms and atomic fragments crossing the bubble and (ii) damage assisted resolution, which occurs from the thermally activated incorporation of helium atoms into disordered regions of the lattice. We discuss here the impact of these two observations upon models of gas resolution in pure crystalline UO_2.

For small gas bubbles (first example, shown in Fig. 1) radiation enhanced resolution resulted in a significant fraction of the helium gas atoms being removed from the bubble into the UO_2 lattice. On the timescales of these simulations some of these atoms end up at interstitial sites in a recrystallised portion of the lattice, while others are within the still disordered lattice region adjacent to the bubble.

Larger, less gas-dense bubbles exhibit much lower relative levels of resolution (i.e. helium atoms returned to the lattice as a proportion of the total number of helium atoms). This is primarily because the rates of resolution via the two mechanisms will depend upon the density of gas atoms within the bubble. For damage assisted resolution the rate (for a given gas-density) will depend upon the surface area of the bubble intersected by the cascade

Table 2
Levels of resolution (in helium atoms resolved per cascade) calculated from molecular dynamics simulations of cascade damage interaction with helium bubbles at several different gas densities, details of the method of calculation are given in the text

No. He atoms	Atomic density Per UO_2	Pressure MPa	No. resolved He atoms Total	Thermal	Ballistic
250	0.31	22	2.2(1.8)	0.3(0.5)	1.8(1.7)
500	0.61	53	2.5(2.6)	1.2(1.1)	1.3(1.6)
750	0.91	71	7.4(5.2)	2.4(2.0)	5.0(3.2)
1000	1.22	98	8.3(5.5)	5.0(4.2)	3.3(1.6)
1250	1.52	125	10.5(5.5)	5.3(3.0)	5.2(2.73)
1500	1.83	153	25.7(11.5)	10.7(5.4)	15.0(6.7)
1712	2.08	180	30.0(8.7)	12.7(3.4)	17.3(5.25)

Numbers in brackets refer to one standard deviation. We also report equivalent gas pressures for helium in a free gas.

damage, since it is only atoms at the surface that have access to the disordered lattice region. For ballistic recoil, the resolution rate will depend upon the probability of a high-energy species encountering a helium gas atom within the bubble void. However, for larger bubbles the free path of energetic gas atoms within the bubble void may be smaller than the size of the bubble. In this case even if ballistic gas atoms within the void are created they will not necessarily reach the surface of the bubble due to the rapid loss of energy due to collisions with other gas atoms. Consequently, for sufficiently large bubbles, of order of several tens of nanometers, it is suggested that ballistic recoil resolution will also be a surface phenomenon. Such a case is more likely too occur in krypton and xenon gas bubbles as these have a far higher pressure and lower mean free path than the helium examples considered here.

Acknowledgements

This work was carried out as part of the TSEC programme KNOO and as such we are grateful to the EPSRC for funding under Grant EP/C549465/1. Calculations were performed on the Imperial College High Performance Computing Service [43]. We would also like to thank Simon Burbidge for helpful discussion on the running of these calculations.

References

[1] W. Nixon, D.A. Machinnes, J. Nucl. Mater. 101 (1981) 192.
[2] R.W. Grimes, R.H. Miller, C.R.A. Catlow, J. Nucl. Mater. 172 (1990) 123.
[3] V. Chkuaseli, H. Matzke, J. Nucl. Mater. 201 (1993) 92.
[4] S. Guilbert, T. Sauvage, H. Erramli, M.-F. Barthe, P. Desgardin, G. Blondiaux, C. Corbel, J. Piron, J. Nucl. Mater. 321 (2003) 121.
[5] G. Sattonnay, L. Vincent, F. Garrido, L. Thome, J. Nucl. Mater. 355 (2006) 131.
[6] K. Une, J. Nucl. Mater. 158 (1988) 188.
[7] R.F. Hillbert, V.W. Storhok, W. Chubb, D.L. Keller, J. Nucl. Mater. 38 (1971) 26.
[8] C. Ferry, C. Poinssot, C. Cappelaere, L. Desgranges, C. Jegou, F. Miserque, J. Piron, D. Roudil, J. Gras, J. Nucl. Mater. 352 (2006) 246.
[9] B. Buescher, R. Meyer, J. Nucl. Mater. 48 (1973) 143.
[10] M.O. Tucker, J. Nucl. Mater. 78 (1978) 17.
[11] C.T. Walker, P. Knappik, M. Mogensen, J. Nucl. Mater. 160 (1988) 10.
[12] U.M. El-Saied, D.R. Olander, J. Nucl. Mater. 207 (1993) 313.
[13] M. Veshchunov, J. Nucl. Mater. 277 (2000) 67.
[14] C. Baker, J. Nucl. Mater. 71 (1977) 117.
[15] W. Chubb, J. Nucl. Mater. 91 (1980) 240.
[16] V. Chkuaseli, H. Matzke, J. Nucl. Mater. 223 (1995) 61.
[17] J.H. Evans, A. van Veen, J. Nucl. Mater. 252 (1998) 156.
[18] G.P. Tiwari, J. Nucl. Mater. 252 (1998) 156.
[19] J. Evans, A. van Veen, K. Westerduin, J. Nucl. Mater. 195 (1992) 250.
[20] J.A. Turnbull, R.M. Cornell, J. Nucl. Mater. 36 (1970) 161.
[21] O. Gautsch, J. Nucl. Mater. 35 (1970) 109.
[22] C. Ronchi, P.T. Elton, J. Nucl. Mater. 140 (1986) 228.
[23] M. Abramowski, R.W. Grimes, S. Owens, J. Nucl. Mater. 275 (1999) 12.
[24] D.E. Beck, Mol. Phys. 14 (4) (1968) 311.
[25] W. Smith, C. Yong, P. Rodger, Mol. Simul. 28 (2002) 385.
[26] W. Smith, I. Todorov, The DLPOLY 3.0 User Manual, Daresbury Laboratory, UK.
[27] H.J.C. Berendsen, J.P.M. Postma, W. van Gunsteren, A. DiNola, J.R. Haak, J. Chem. Phys. 81 (1984) 3684.
[28] S.A. Adelman, J. Doll, J. Chem. Phys. 64 (1976) 2375.
[29] M.P. Allen, D.J. Tildesley, Computer Simulation of Liquids.
[30] J.F. Ziegler, J.P. Biersack, U. Littmark, The Stopping and Range of Ions in Solids, vol. 1, Pergamon, New York, 1985.
[31] M.J. Cooper, Acta Crystallogr. Sect. B: Struct. Sci. 38 (1982) 264.
[32] P.S. Maiya, Acta Metall. 19 (1971) 255.
[33] S.M. Valone, M.I. Baskes, R.L. Martin, Phys. Rev. B: Condens. Matter 73 (2006) 214209.
[34] I.R. Brearley, D.A. MacInnes, J. Nucl. Mater. 95 (3) (1980) 239.
[35] K. Kamimura, Y. Kobayashi, T. Nomata, In: Proceedings of the IAEA International Symposium in MOX Fuel Cycle Technologies for Medium and Long Term Deployment, Vienna, 1999.
[36] F. Lemoine, J. Nucl. Sci. Technol. 43 (2006) 1105. No. 9 Special Issue on Water Reactor Fuel Performance.
[37] J. Yoo, Y. Oka, Y. Ishiwatari, J. Liu, Ann. Nucl. Eng.
[38] J.P. Piron, M. Pelletier, J. Pavageau, Helium behaviour in spent UO_2 and MOX fuels, No. 311 in Fission Gas Behaviour in Water Reactor Fuels, Vienna, 2000.
[39] P. Garcia, P. Martin, G. Carlot, E. Castelier, M. Ripert, C. Sabathier, C. Valot, F. DAcapito, J.-L. Hazemann, O. Proux, V. Nassif, J. Nucl. Mater. 352 (2006) 136.
[40] K. Nogita, K. Une, Nucl. Instrum. and Meth. B 141 (1998) 481.
[41] L. Van Brutzel, J.M. Delaye, M. Rarivomanantsoa, D. Ghaleb, Philos. Mag. 83 (36) (2003) 4083.
[42] L. Van Brutzel, M. Rarivomanantsoa, D. Ghaleb, J. Nucl. Mater. 354 (1–3) (2006) 28.
[43] Url: <http://www.imperial.ac.uk/ict/services/teachingandresearchservices/highperformancecomputing>.